MIT Open Access Articles

Control of Eukaryotic Cell Migration Through Modulation of Extracellular Chemoattractant Gradients

Massachusetts Institute of Technology

DSCC2010-(% $

CONTROL OF EUKARYOTIC CELL MIGRATION THROUGH MODULATION OF EXTRACELLULAR CHEMOATTRACTANT GRADIENTS

Waleed A. Farahat
Department of Mechanical Engineering
Massachusetts Institute of Technology
Cambridge, Massachusetts 02139
Email: wfarahat@mit.edu

H. Harry Asada
Department of Mechanical Engineering
Massachusetts Institute of Technology
Cambridge, Massachusetts 02139
Email: asada@mit.edu

ABSTRACT

Cell migration is fundamental to a wide range of biological and physiological functions including: wound healing, immune defense, cancer metastasis, as well as the formation and development of biological structures such as vascular and neural networks. In these diverse processes, cell migration is influenced by a broad set of external mechanical and biochemical cues, particularly the presence of (time dependent) spatial gradients of soluble chemoattractants in the extracellular domain. Many biological models have been proposed to explain the mechanisms leading to the migratory response of cells as a function of these external cues. Based on such models, here we propose approaches to controlling the chemotactic response of eukaryotic cells by modulating their micro-environments in vitro (for example, using a microfluidic chemotaxis chamber). By explicitly modeling i) chemoattractant-receptor binding kinetics, ii) diffusion dynamics in the extracellular domain, and iii) the chemotactic response of cells, models for the migration processes arise. Based on those models, optimal control formulations are derived. We present simulation results, and suggest experimental approaches to controlling cellular motility in vitro, which can be used as a basis for cellular manipulation and control.

INTRODUCTION

Cell migration and motility is fundamental to many biological and physiological processes. Simple bacteria, such as *E. Coli*, swim by adaptively modulating flagellar tumbling and turning rates. This enables swimming towards favorable environments, which leads to survival and prosperity of the bacterial and colony [1]. Complex eukaryotic cells migrate by constantly remodeling their cytoskeletons to achieve a wide arrange of key

biological functions. For example, in the context of structural development, endothelial tip cells guide the formation of vascular sprouts achieve viable capillary networks [2], whereas neural growth cones guide axonal migration that is necessary for forming neural interconnections [3]. In the context of wound healing, epithelial cells migrate towards wound sites to build protective barriers, while neutrophils migrate to chase invading bacteria and microbes, eventually engulfing and digesting them in an important defense mechanism [4]. In the context of cancer metastasis, tumor cell migration is a necessary step for intravasation into the capillary vessels [5], eventually leading to its transport via blood into far reaching locations in the body. Common to all of these diverse examples is the premise that cells migrate in response to extracellular environmental cues. These cues can be either one or a combination of the following factors: i) the presence of gradients of soluble growth factors or chemoattractants that initiate and guide cell movement along gradient directions, ii) the presence of insoluble molecules bound to the extra cellular matrix that also influence the cell's trajectory, and iii) the presence of mechanical interactions between cells and their neighboring cells and extracellular matrix.

Here we study the problem of controlling cell migration by presenting external chemoattractant gradients as environmental cues. These gradients are established by modulating the boundary conditions of a diffusive extracellular region. Consequently, these boundary conditions become control inputs for affecting and guiding the migration process. Eukaryotic cells can sense very shallow gradients (as little as a 2% difference of growth factor concentrations across the cell body). When presented with such a stimulus, cells respond through a complex sequence of signalling activity [6] by switching to a migratory phenotype, and commencing on a continual processes of remodelling their

1

cytoskeletons via polymerization and disassembly of actin filaments [7]. Additionally, the placement and removal of focal adhesion points enable the cells to bind to the extra-cellular matrix, and consequently translocate their cell bodies towards the direction of movement [4]. When cells move in trajectories that are aligned with chemoattractant gradients, the process is known as *chemotaxis*. When cell trajectories are random, and are not directed along the gradients, the migration process is known as *chemokinesis*.

Because *in vivo* cell migration is influenced by a multitude of interacting factors, it is important to address the problem under simplified and well understood physical conditions. Therefore, studying migration under *in vitro* settings that precisely enable control of chemoattractant gradients is desirable. Microfluidic devices are currently being used to achieve this tasks for a variety of settings and cell cultures [8, 9]. While various forms of such devices exist, many consist of a gel region that acts as a surrogate to the extra-cellular matrix. Two channels run along the length of the gel region are used to flow media containing different concentrations of growth factors. Figure 1(a) shows the cross-section schematic of a representative device. The flow rate and composition of this media can be externally controlled via upstream mixers and instrumentation, thereby enabling the control of the concentration of the media at the boundary of the region. The growth factors defuse from the channels into the gel region, and present to the cells with time-varying growth factor concentrations and gradients. The growth factors bind to the receptors differentially along the cell membrane, causing the cells to polarize and migrate. Because the growth factor concentrations are dynamic, they present the cell with gradients in space and time. These gradients induce cytoskeletal remodeling leading to the mechanisms of cell migration. Therefore, to achieve a representative model of the process, diffusion dynamics, in addition to chemoattractant-reception binding kinetics have to be modeled.

The framework described above provides an approach to controlling and manipulating cellular migration *in vitro*. For some problems, it may be desirable to maximize cell migration rates and distances, for example, in the case of maximizing angiogenic sprouting response of endothelial monolayers. This can be cast as an optimal control problem that maximizes a distance traveled metric. In other conditions, it may be desirable to have the cells follow certain paths for patterning and structural formation. This can be viewed as a trajectory control problem.

In this work, we model the problem setting described above, and derive optimal control formulations to guide cell migration. Our objective is to induce and control cellular motion within the gel region by dynamically altering the growth factor concentrations of the media flowing in the channels. In effect, this changes the boundary conditions on the gel region, and therefore the microenvironment presented to the cells.
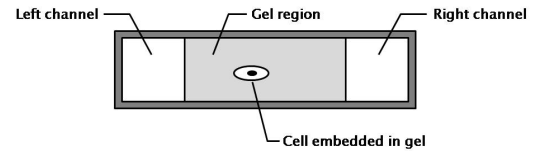
(a) Cross-section of a representative gel region (extra-cellular matrix) bounded by two channels.
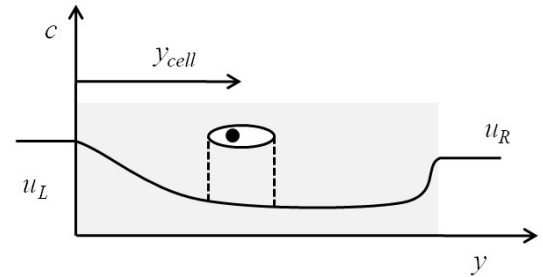
(b) Diffusion region.
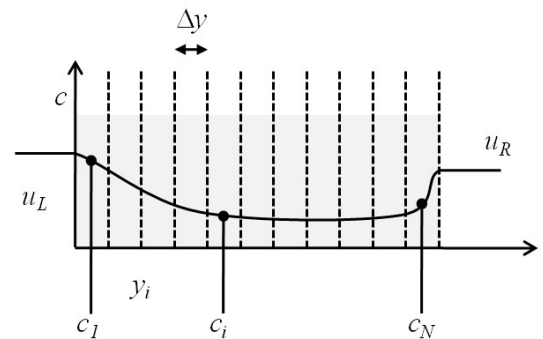
(c) Discretized region.

Figure 1. Problem setup. (a) The concentration profiles ($c(y,t)$) in the 1-dimensional diffusion model is controlled by the concentrations of the media in the left and right channels (u_L and u_R). (b) Discretization of the diffusion problem.

SYSTEM MODEL

We are concerned with the migration of a single cell in a purely diffusive, 1-dimensional homogeneous medium (variations along channel length and height are ignored). The concentration profile in the medium is determined entirely by diffusion, and the time-history of the concentrations of the media at the boundary of the region. Growth factors bind to cell membrane bound receptors, and a certain fraction of the receptors become occupied. Due to the presence of spatial gradients of the chemoattractants, a difference in the fraction of receptors occupied is established between the leading and trailing edges. This difference leads to cell polarization and the initiation of the migratory signaling pathways. Therefore, there are three elements to the system model that are described below: i) diffusion dynamics of the chemoattractants in the extra-cellular domain, ii) growth factor and receptor binding kinetics, and iii) model of cellular responses due the the difference in fraction of receptors occupied.

Diffusion dynamics

Diffusion in the medium is governed by the differential equation

$$\frac{\partial c(y,t)}{\partial t} = D\frac{\partial^2 c(y,t)}{\partial y^2} + R(y,t) \tag{1}$$

where D is the diffusion coefficient (assumed constant throughout the entire region), and $c(y,t)$ is the concentration of the growth factor in the medium at spatial coordinate y and time t. The spatial coordinate considered is one-dimensional and bounded, i.e. $y \in [0,Y]$, since minimal variance along the other channel dimensions. The boundary conditions of this region are $c(0,t) = u_L(t)$ and $c(Y,t) = u_R(t)$. $R(y,t)$ is the reaction rate which can be used to model either growth factor sources (such as when tumors emit chemoattractants) or sinks (such as when cells internalize the chemoattractants). In our model, we assume that the amount of growth factor binding to the cells is negligible compared to the quantities existing in the medium, and therefore we assume $R(y,t) = 0$.

It is convenient to spatially discretize the gel region and write difference equations of the diffusion process. This allows for the diffusion dynamics to be written in an LTI form where the state of the diffusion subsystem is the vector of growth factor concentrations at the discretization grid points. Discretizing over a grid of N points, y_i, with $i \in [1,N]$, the difference approximation of eq. (1) is given by:

$$\frac{\partial c(y_i,t)}{\partial t} = D\frac{\partial^2 c(y_i,t)}{\partial x^2} \approx D\frac{c_{i+1}(t) - 2c_i(t) + c_{i-1}(t)}{(\Delta y)^2} \tag{2}$$

$$\frac{\partial c(y_1,t)}{\partial t} \approx D\frac{c_2(t) - 2c_1(t) + u_L(t)}{(\Delta y)^2} \tag{3}$$

$$\frac{\partial c_N(y_N,t)}{\partial t} \approx D\frac{u_R(t) - 2c_N(t) + c_{N-1}(t)}{(\Delta y)^2} \tag{4}$$

where $\Delta y = N/Y$ is the grid spacing. Based on this difference approximation, the following state representation of the diffusion dynamics is written:

$$\begin{Bmatrix} \dot{c}_1 \\ \dot{c}_2 \\ \vdots \\ \dot{c}_N \end{Bmatrix} = \frac{D}{(\Delta y)^2}\begin{bmatrix} -2 & 1 & & & \\ 1 & -2 & 1 & & \\ & 1 & -2 & 1 & \\ & & \ddots & \ddots & \ddots \\ & & & 1 & -2 & 1 \end{bmatrix}\begin{Bmatrix} c_1 \\ c_2 \\ \vdots \\ c_N \end{Bmatrix} +$$

$$\frac{D}{(\Delta y)^2}\begin{bmatrix} 1 & 0 \\ 0 & 0 \\ \vdots & \vdots \\ 0 & 1 \end{bmatrix}\begin{Bmatrix} u_L \\ u_R \end{Bmatrix} \tag{5}$$

Equation (5) can be compactly written as

$$\dot{\mathbf{c}} = \mathbf{A}_c\mathbf{c} + \mathbf{B}_c\mathbf{u}_c \tag{6}$$

Receptor-growth factor binding kinetics

The kinetics of the growth factor (which is the ligand, L, in this case) and the membrane bound receptor (R), into a product (P) of an occupied receptor (as illustrated in fig. 2):

$$[L] + [R] \rightleftharpoons [P] \tag{7}$$
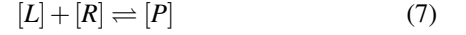
The dynamics of this interaction are driven by the law of mass action, which can be written in differential equation form as follows:

$$\frac{d[P]}{dt} = k_{on}[L][R] - k_{off}[P] \tag{8}$$

where k_{on} and k_{off} are the forward and backward reaction rates respectively, and the notation $[\cdot]$ denotes the concentration of the argument. Assuming steady-state conditions of the binding kinetics, the derivative terms vanish, leading to:

$$0 = k_{on}[L][R] - k_{off}[P] \tag{9}$$

$$[P] = \frac{1}{k_D}[L][R] \tag{10}$$

where $k_D = k_{off}/k_{on}$ is the reaction disassociation constant. The steady-state assumption is justifiable because the reaction binding kinetics of the growth factor and receptor typically reach steady state within a few micro-seconds for such proteins, whereas meaningful cellular migration time scales are typically on the order of hours.

The fraction of receptors occupied (FRO) in any region of the cell membrane is therefore given by

$$\begin{aligned} \text{FRO} = \frac{[P]}{[P]+[R]} &= \frac{[R][L]/k_D}{[R][L]/k_D + [R]} \\ = \frac{[L]}{[L]+k_D} &= \frac{c(y,t)}{c(y,t)+k_D} \end{aligned} \tag{11}$$

where the last equality follows since $c(y,t)$ is the concentration of the growth factor, or the ligand (L). The difference in fraction of receptors occupied between the leading and trailing edge of the cell. The location of the leading edge of the cell is given by $y+w$, while the location of the trailing edge is given by $y-w$. Therefore, we write

$$u_\delta(t) = \frac{c(y+w,t)}{c(y+w,t)+k_D} - \frac{c(y-w,t)}{c(y-w,t)+k_D} \tag{12}$$
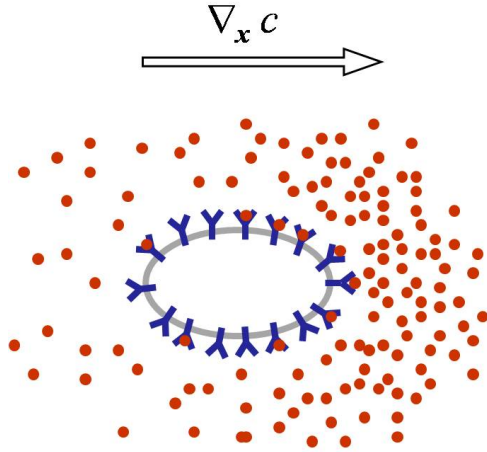
3

Figure 2. Illustration of ligand (red circles) binding to membrane bound receptors (blue) in the presence of a ligand concentration gradient. As a result, the fraction of receptors occupied on the right side is greater than the fraction of receptors occupied on the left side.

Since the concentrations at the leading and trailing edges of the cells depend on cell locations, means for interpolating the concentrations as a function of the concentrations at the grid point locations c_i are necessary. We rely on Gaussian radial basis functions to ensure smoothness of the interpolating functions (linear interpolations are necessarily discontinuous). Thus, the interpolated concentration for an arbitrary location y is given by

$$c(y,t) = \sum_{i=1}^{N} c_i(t) \cdot e^{-\left(\frac{y_i-y}{\sigma}\right)^2} = \mathbf{c}^T(t) \cdot \mathbf{d}(y_{cell}) \qquad (13)$$

where y_i is the grid coordinate, and σ is the spread of the Gaussian radial basis function, and the ith element of the vector $\mathbf{d}$ is $e^{-\left(\frac{y_i-y}{\sigma}\right)^2}$.

Cell migration model

To model the response of the cell as a function of the difference in fraction of receptors occupied, we rely on a migration model presented in [10]. In this model, cell motion is driven by a random noise component, a chemotactic component, and an autoregressive (damping-like) term. Modifying this model to our problem setting, and focusing on the deterministic aspects of the model, we write:

$$\ddot{y}_{cell} = -\beta \dot{y}_{cell} + \kappa \cdot u_\delta \qquad (14)$$

where β is the autoregressive velocity term, and κ is known as the chemotactic responsiveness of the cell. While this model can be viewed as highly simplistic, it has been shown to reproduce cell migration patterns in a qualitatively similar way to experimental observations [10].

Integrated System Model

To integrate equations (6), (12), and (14) into a common system model, it is useful to expand the input state vector to include various intermediate variables as fictitious control inputs. We expand the control input vector, and write

$$\mathbf{u} = \begin{Bmatrix} u_L \\ u_R \\ u_\delta \\ u_{CL} \\ u_{CR} \end{Bmatrix} = \begin{Bmatrix} u_L \\ u_R \\ u_\delta \\ c(y_{cell}-w) \\ c(y_{cell}+w) \end{Bmatrix} \qquad (15)$$

where the definitions of the various quantities are self-evident. This allows us to write the dynamics of the system in the following LTI form:

$$\begin{Bmatrix} | \\ \dot{\mathbf{c}} \\ | \\ \hline \ddot{y}_{cell} \\ \dot{y}_{cell} \end{Bmatrix} = \begin{bmatrix} & & \vdots & \\ & \mathbf{A}_c & & 0 \\ & & \vdots & \\ \hline & & -\beta & 0 \\ \cdots & 0 & \cdots & 1 & 0 \end{bmatrix} \begin{Bmatrix} | \\ \mathbf{c} \\ | \\ \hline \dot{y}_{cell} \\ y_{cell} \end{Bmatrix} +$$

$$\begin{bmatrix} D/(\Delta y)^2 & 0 & \vdots & \vdots & \vdots \\ 0 & \vdots & 0 & 0 & 0 \\ \vdots & & \vdots & \vdots & \vdots \\ & D/(\Delta y)^2 & & & \\ \hline 0 & 0 & \kappa & 0 & 0 \\ 0 & 0 & 0 & 0 & 0 \end{bmatrix} \begin{Bmatrix} u_L \\ u_R \\ u_\delta \\ u_{CL} \\ u_{CR} \end{Bmatrix} \qquad (16)$$

Because the 5×1 input vector $\mathbf{u}$ has been expanded from the 2×1 vector $\mathbf{u}_c$, algebraic constraints relating the control inputs have to be satisfied. Specifically:

$$u_\delta = \frac{u_{CR}}{u_{CR}+k_D} - \frac{u_{CL}}{u_{CL}+k_D} \qquad (17)$$

$$u_{CL} = \sum_{i=1}^{N} c_i \cdot e^{-\left(\frac{y_i-(y_{cell}-w)}{\sigma}\right)^2} = \mathbf{c}^T \cdot \mathbf{d}_L(y_{cell}) \qquad (18)$$

$$u_{CR} = \sum_{i=1}^{N} c_i \cdot e^{-\left(\frac{y_i-(y_{cell}+w)}{\sigma}\right)^2} = \mathbf{c}^T \cdot \mathbf{d}_R(y_{cell}) \qquad (19)$$

4

In summary, equations (16) to (19) can be compactly written as

$$\dot{\mathbf{x}} = \mathbf{A}\mathbf{x} + \mathbf{B}\mathbf{u} \tag{20}$$

$$\text{s.t.} \quad \mathbf{g}(\mathbf{x}, \mathbf{u}) = \mathbf{0} \tag{21}$$

In this compact form, it becomes apparent that the model assumes a Hammerstein-like model structure as depicted in fig. 3.
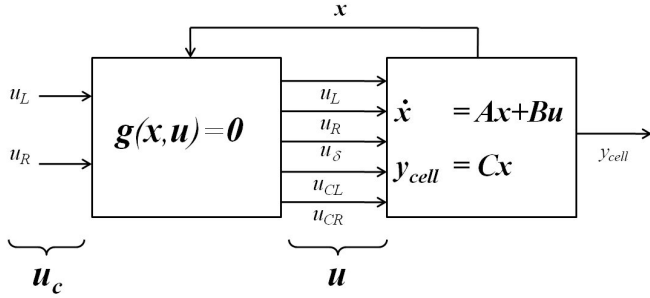

Figure 3. A Hammerstein-like model representation of the cell migration process.

Open-loop Simulations

Open-loop simulations illustrating the system response are shown in Figure 4. The Figure shows the time evolution of the concentration gradients in the extracellular domain, and the resulting cell trajectories. Simulations are shown for different input concentrations at the left and right boundary channels, including: constant levels (4(a)), linear ramps (4(b)), sinusoidal (4(c)) and square inputs (4(d)). The values of the simulation parameters were chosen to replicate the dynamics of the Vascular Endothelial Growth Factor (VEGF) diffusion through a medium of collagen, and the binding kinetics to the VEGF receptor on endothelial cells. These parameters are: $D = 5 \times 10^{-11}$ [m²/s], $k_D = 1 \times 10^{-9}$ [M] and cell dimensions of approximately 50 [microns]. All simulations start at zero concentration levels in the extracellular domain, and with the cells adjacent to the left channel.

The simulations suggest an interesting outcome: if maximal migration velocities are desired, extremal controls are not necessarily optimal. For example, in Figure 4(a), the chemoattractant concentration at the right channel was maintained at a maximal value of 50 ng/mL at all times, whereas the corresponding concentration in Figure 4(b) was a linearly increasing ramp leading up to 50 ng/mL only after 10 hours. Even though the chemoattractant input in Figure 4(b) was less, the cells responded more rapidly by traveling across the domain in less time. This perhaps counter-intuitive result motivates the need to cast the migration control problem in an optimal control framework, which is discussed next.

AN OPTIMAL CONTROL FORMULATION

We propose an optimal control formulation relying on the Pontryagin Minimum Principle [11] to enable cell trajectory control as it migrates through the diffusion medium. The cost function formulation is given by:

$$\mathbf{u}^* = \arg\min_{\mathbf{u}} \left\{ \varphi(\mathbf{x}|_{t=T}) + \int_0^T \mathcal{L}(\mathbf{x}, \mathbf{u}) \mathbf{dt} \right\} \tag{22}$$

. We chose a general Lagrangian cost function is given by

$$\mathcal{L} = \frac{\alpha}{2} \left(y_{cell} - y_{des} \right)^2 + \frac{\gamma}{2} \left(u_L^2 + u_R^2 \right) + \upsilon \tag{23}$$

and the terminal cost that maximizes net cell migration

$$\varphi(\mathbf{x}|_{t=T}) = -y_{cell} = -x_{N+2} \tag{24}$$

This cost function can be specialized to various cases via appropriate parameter settings. For example, in most practical cases, there is no cost associated with the control inputs u_L and u_R since they represent chemoattractant concentrations. This can be captured by setting $\gamma = 0$. Similarly, if cell trajectory following is desired, we set all coefficients other than α to zero. If minimum travel time from extremal points is desired, we set all coefficients other than υ to zero.

We define the Hamiltonian scalar function $\mathcal{H}$ as

$$\mathcal{H} = \lambda^T \mathbf{f}(\mathbf{x}, u) + \mathcal{L}(\mathbf{x}, \mathbf{u}) + \mu^T \mathbf{g}(\mathbf{x}, \mathbf{u}) \tag{25}$$

where the $(N+2) \times 1$ co-states vector λ includes the Lagrange multipliers associated with the dynamic constraint (20) and the 3×1 vector $\mu = [\mu_\delta, \mu_{CL}, \mu_{CR}]^T$ includes the Lagrange multipliers associated with the algebraic input control constraints (17), (18), and (19).

From the Pontryagin Minimum Principle, the optimal control and optimal trajectories are characterized by:

$$\dot{\lambda}^* = -\nabla_{\mathbf{x}} \mathcal{H} \tag{26}$$

$$\mathbf{u}^* = \arg\min_{\mathbf{u}} \left\{ \mathcal{H} \right\} \tag{27}$$

where $(\cdot)^*$ denotes quantity optimality. Equation (26) can be used to characterize the optimal co-states trajectories $\lambda^*(t)$. Equation 27, is used the define the optimal controls. In most cases it can be equivalently characterized by $\nabla_{\mathbf{u}} \mathcal{H} = 0$, thereby defining 5 constraints. Two of these constraints are used to define the real control inputs (u_L, u_R), while the remaining three constraints define the multipliers $(\mu_\delta, \mu_{CL}, \mu_{CR})$. The first two relations define the optimal control inputs as follows:
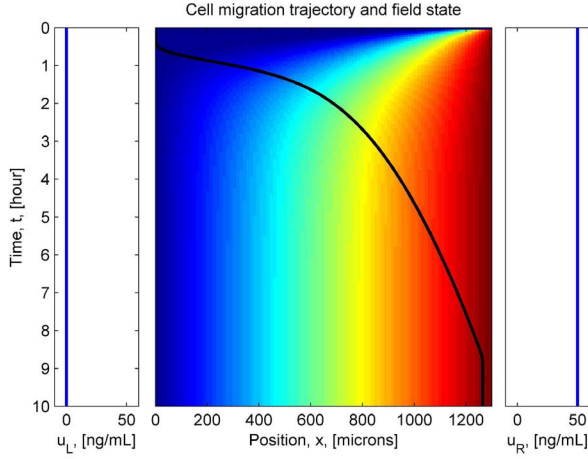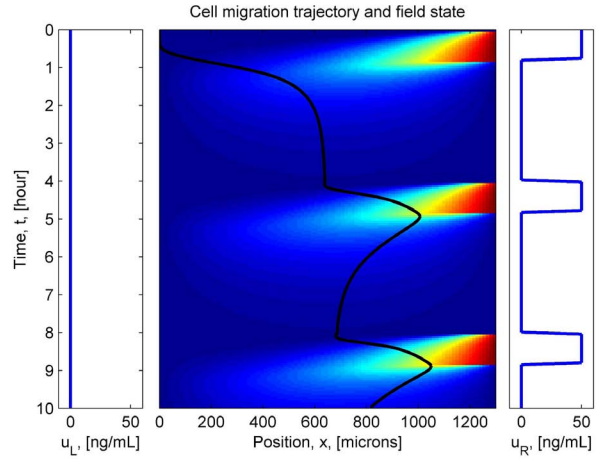
(a) Zero input at left channel, constant input at right channel.
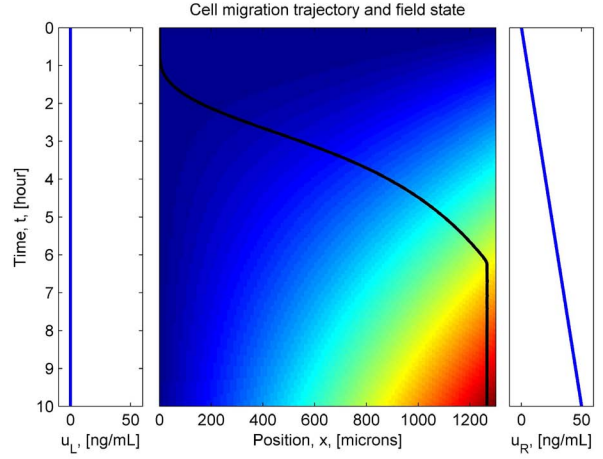
(b) Zero input at left channel, linear input at right channel.
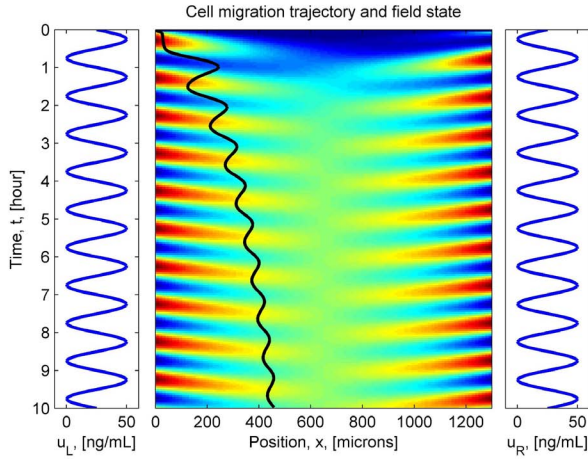
(c) Sinusoidal input at both channels.

(d) Zero input at left channel, Square input at right channel.

Figure 4. Simulation results showing the input concentrations at the left channel, right channel, and the time evolution of the field concentration long time. The location of the cell is initiated at the left end of the field. The cell trajectory is illustrated by the black line. (a) Constant concentrations applied ($U_l = 0$ and $u_R = 50$ for all time). (b) Linearly ramping concentrations in the right channels. (c) Sinusoidal concentrations on both channels. (d) Pulsatile concentrations on the right channel.

$$\frac{\partial \mathcal{H}}{\partial u_L} = \frac{D}{(\Delta y)^2}\lambda_1 + \gamma u_L$$

$$\Rightarrow u_L^* = \begin{cases} u_{L_{max}} & \text{if } -\frac{\lambda_1}{\gamma}\frac{D}{(\Delta y)^2} > u_{L_{max}} \\ -\frac{\lambda_1}{\gamma}\frac{D}{(\Delta y)^2} & \text{if } u_{L_{min}} < -\frac{\lambda_1}{\gamma}\frac{D}{(\Delta y)^2} < u_{L_{max}} \\ u_{L_{min}} & \text{if } -\frac{\lambda_1}{\gamma}\frac{D}{(\Delta y)^2} < u_{L_{min}} \end{cases} \quad (28)$$

and

$$\frac{\partial \mathcal{H}}{\partial u_R} = \frac{D}{(\Delta y)^2}\lambda_N + \gamma u_R$$

$$\Rightarrow u_R^* = \begin{cases} u_{R_{max}} & \text{if } -\frac{\lambda_N}{\gamma}\frac{D}{(\Delta y)^2} > u_{R_{max}} \\ -\frac{\lambda_1}{\gamma}\frac{D}{(\Delta y)^2} & \text{if } u_{R_{min}} < -\frac{\lambda_N}{\gamma}\frac{D}{(\Delta y)^2} < u_{R_{max}} \\ u_{R_{min}} & \text{if } -\frac{\lambda_N}{\gamma}\frac{D}{(\Delta y)^2} < u_{R_{min}} \end{cases} \quad (29)$$

Note that in cases when $\gamma = 0$, optimal controls u_L^* and u_R^* take the form of *bang-bang* control. This is primarily due to the

6

Copyright © 2010 by ASME

Hamiltonian not being a function of the inputs. The remaining three relations define the multipliers μ as follows:

$$\frac{\partial \mathcal{H}}{\partial u_\delta} = \lambda_{N+1}\kappa + \frac{\partial \mathcal{L}}{\partial u_\delta} + \mu_\delta$$
$$\Rightarrow \quad \mu_\delta^* = -\lambda_{N+1}\kappa \tag{30}$$

$$\frac{\partial \mathcal{H}}{\partial u_{CL}} = \frac{\partial \mathcal{L}}{\partial u_{CL}} + \mu_\delta \frac{k_D}{(u_{CL}+k_D)^2} + \mu_{CL}$$
$$\Rightarrow \quad \mu_{CL}^* = \frac{\lambda_{N+1}\kappa k_D}{(u_{CL}+k_D)^2} \tag{31}$$

$$\frac{\partial \mathcal{H}}{\partial u_{CR}} = \frac{\partial \mathcal{L}}{\partial u_{CR}} - \mu_\delta \frac{k_D}{(u_{CR}+k_D)^2} + \mu_{CR}$$
$$\Rightarrow \quad \mu_{CR}^* = -\frac{\lambda_{N+1}\kappa k_D}{(u_{CR}+k_D)^2} \tag{32}$$

Finally, the optimal costate trajectories are given by:

$$\dot{\lambda}^* = -\mathbf{A}^T\lambda - \nabla_{\mathbf{x}}\mathcal{L} - \mu_{CL}\left\{ \nabla_{\mathbf{x}}\mathbf{d}_L \cdot \mathbf{c} + \begin{bmatrix} \mathbf{d}_L \\ 0 \end{bmatrix} \right\}$$
$$- \mu_{CR}\left\{ \nabla_{\mathbf{x}}\mathbf{d}_R \cdot \mathbf{c} + \begin{bmatrix} \mathbf{d}_R \\ 0 \end{bmatrix} \right\} \tag{33}$$

where

$$\nabla_{\mathbf{x}}\mathcal{L} = [0, \cdots, 0, \alpha(y_{cell} - y_{des})]^T$$

Thus, to solve for the optimal controls, state trajectories, costate trajectories and Lagrange multipliers, equations (28) - (33) have to be solved simultaneously. The boundary conditions of the solutions are given by

$$\mathbf{x}(t=0) = \mathbf{0} \tag{34}$$
$$\lambda(t=T) = \nabla_{\mathbf{x}} \cdot \varphi(t=T)$$
$$= [0, 0, \cdots, 0, -1] \tag{35}$$

These equations and the boundary conditions characterize the optimal trajectories.

CONCLUSIONS

We presented a model and an approach to the problem of controlling cell migration. A key feature of eukaryotic cell migration is that migration velocities depend on the difference of fraction of receptors occupied. A simple growth factor-receptor binding kinetics model reveals that the inputs are transformed nonlinearly to what is otherwise assumed to an LTI process. We developed a Hammerstein-like model of this process. Simulations showed that in order to maximize cell migration rates across a region, extremal controls are not necessarily optimal. This motivated the derivation of optimal control conditions by relying on the Pontryagin minimum principle.

REFERENCES

[1] Alon, U., Surette, M. G., Barkai, N., and Leibler, S., 1998. "Robustness in bacterial chemotaxis". *Nature,* **397**, pp. 168–171.

[2] Barkefors, I., Le Jan, S., Jakobsson, L., Hejll, E., Carlson, G., Johansson, H., Jarvius, J., Park, J. W., Li Jeon, N., and Kreuger, J., 2008. "Endothelial Cell Migration in Stable Gradients of Vascular Endothelial Growth Factor A and Fibroblast Growth Factor 2". *Journal of Biological Chemistry,* **283**(20), pp. 13905–13912.

[3] Huber, A. B., Kolodkin, A. L., Ginty, D. D., and Cloutier, J.-F., 2003. "Signaling at the growth cone: Ligand-receptor complexes and the control of axon growth and guidance". *Annual Review of Neuroscience,* **26**(1), pp. 509–563.

[4] Lodish, H., Berk, A., Kaiser, C., Krieger, M., Scott, M., Bretscher, A., Ploegh, H., and Matsudaira, P., 2008. *Molecular Cell Biology*, sixth ed. W. H. Freeman and Company.

[5] Folkman, J., 2007. "Angiogenesis: an organizing principle for drug discovery?s". *Nature Reviews,* **6**, pp. 273–286.

[6] Levchenko, A., and Iglesias, P. A., 2002. "Models of eukaryotic gradient sensing: Application to chemotaxis of amoebae and neutrophils". *Biophysical Journal,* **82**(1), pp. 50 – 63.

[7] Pollard, T. D., and Borisy, G. G., 2003. "Cellular motility driven by assembly and disassembly of actin filaments". *Cell,* **112**(4), pp. 453 – 465.

[8] Chung, S., R.Sudo, P. J. Mack, P., Wan, C., Vickerman, V., and Kamm, R. D., 2009. "Cell migration into scaffolds under co-culture conditions in a microfluidic platform.". *Lab Chip,* **9**, pp. 269–275.

[9] Wang, S.-J., Saadi, W., Lin, F., Nguyen, C. M.-C., and Jeon, N. L., 2004. "Differential effects of egf gradient profiles on mda-mb-231 breast cancer cell chemotaxis". *Experimental Cell Research,* **300**(1), pp. 180 – 189.

[10] Stokes, C., Lauffenburger, D., and Williams, S., 1991. "Migration of individual microvessel endothelial cells: stochas-

tic model and parameter measurement". *J Cell Sci,* **99**(2), pp. 419–430.

[11] Bryson, A. E., and Ho, Y.-C., 1975. *Applied Optimal Control: Optimization, Estimation and Control*. John Wiley & Sons, New York.